



Influence of Side Chain on the Inhibition of Aluminium Corrosion in HCl by α -Amino Acids

Najib U. Shehu, Umar Ibrahim Gaya* and A. A. Muhammad

Department of Pure and Industrial Chemistry, Faculty of Physical Sciences, Bayero University, Kano, Nigeria

* Corresponding author. E-mail: uigaya.chm@buk.edu.ng DOI: 10.14416/j.asep.2019.07.002

Received: 13 April 2019; Revised: 31 May 2019; Accepted: 7 June 2019; Published online: 5 July 2019

© 2019 King Mongkut's University of Technology North Bangkok. All Rights Reserved.

Abstract

Aside from functional groups, aromatic rings have mostly been regarded as zones via which certain inhibitors can protect etching metal parts. Substituent groups generally can be aromatic or non-aromatic, comparison of which is scanty in literature. Among these, amino acids exhibit side substituent chain in addition to amino- and carboxylic carbonyl- functional groups, hence may show unique behaviours in corrosive environment. The side chains of amino acids can vary from H- to alkyl and then to aromatic. This study is devoted to the investigation of the influence of non-polar, hydrophobic side chain of amino acid homologues (glycine, alanine and phenylalanine) on the inhibition of aluminium corrosion in 0.3 M HCl. Corrosion properties and inhibition mechanism were analysed using mass loss, solid-state characterisation and quantum chemical methods. Potentiodynamic polarisation results confirmed cathodic inhibition, which was relatively less efficient with glycine and phenylalanine. The adsorption of these inhibitors was consistent with Langmuir isotherm and physical mechanism. Activation parameters, topography, electropotential shifts quantum studies and mass loss confirmed the superiority of the inhibiting effect of alanine. It is therefore argued herein that the aromatic carbocyclic moiety of phenylalanine does not dictate its anti-corrosion effect in acidic media, but preferentially, properties such as the adsorption type, corrosion medium, interfacial behaviour of adsorbates and temperature.

Keywords: Aluminium, Corrosion, Adsorption, DFT, Amino acid

1 Introduction

Much as iron, aluminium is globally widespread in application, and as a less noble non-ferrous metal it has a strong tendency to undergo all forms of corrosion in different environments. The extraction of this metal from bauxite is energy intensive and relatively expensive [1], necessitating the need for protection against severe corrosion problems. Nowadays, the use of acidic media in pickling, facility cleaning and descaling is indispensable in some many industries [2], [3]. Hydrochloric acid is a common acidic medium for these purposes because it is more economical, efficient and less troublesome compared to other mineral acids

[4]. Even though aluminium is effectively passive in neutral aqueous solutions, it is strongly predisposed to corrosion in acidic media even as dilute as acid rainwater [5]. In actual fact, Cl⁻ from various sources, including neutral salts, has the ability to cause pitting corrosion at vulnerable spots of passive film-protected non-ferrous metals.

Aluminium has been successfully protected against corrosion by anodising, painting, coating, cathodic protection, application of inhibitors and by chemical treatment with inorganic salts such as chromates. Basically, depending upon the protection method, the thin, 0.05 to \approx 0.15 μ m oxide film is replaced by a thicker, 50 to 120 μ m complex layer [6].

Please cite this article as: N. U. Shehu, U. I. Gaya, and A. A. Muhammad, "Influence of side chain on the inhibition of aluminium corrosion in HCl by α -amino acids," *Applied Science and Engineering Progress*, vol. 12, no. 3, pp. 186–197, Jul.–Sep. 2019.

Chromate conversion coatings and chromate inhibitors are still the best and most efficient corrosion inhibitors but these are not environmentally friendly due to their toxicity and carcinogenicity. On the other hand, a wide range of inhibitors offers desirable attributes such as non-toxicity, a variety of choices and ready availability. However, they cannot universally protect all metals in the same aggressive media, thus prompting the search for efficient metal or medium-specific inhibitors. Consequently, organic inhibitors of various classes have been the subject of intensive research interest as potential materials for the surface protection of ferrous and non-ferrous metals and their alloys against aggressive environments [7]–[10].

The performance of adsorption-type organic inhibitors is influenced by the presence of a hydrophobic hydrocarbon part, hydrophilic functional groups (such as $-\text{NH}_2$, $-\text{SH}$, $-\text{OH}$, $-\text{COOH}$, $-\text{C}=\text{O}$, $-\text{N}=\text{N}$, $-\text{PO}_3^{3-}$ or their derivatives), aromatic rings, molecular area, molecular weight, temperature and electrochemical potential at the metal/solution interface [11], [12]. Capitalising on the preference for compounds or matrices with low or non-toxicity [13], myriad well-performing organic and organometallic inhibitors have been reported for aluminium which includes organic Schiff bases [14], plant extracts [15], [16], dyes [3], pharmaceuticals [17] and heterocyclics [18]. Amino acids particularly, have at least two of the aforementioned functional groups ($-\text{NH}_2$ and $-\text{COOH}$) and may exhibit aromatic ring, so when used as inhibitors they afford easy dissolution and facile binding to the metal surface and blockage of active sites. In addition, this class of inhibitors is cost-effective, water-soluble, non-toxic and biodegradable.

There is no shortage of literature on utilization of a wide range of amino acids such as glutamic acid, cysteine, histidine, glycine (Gla), alanine (Ala), phenylalanine (Phe), leucine, their derivatives, or their combinations, for inhibition of corrosion of different metals such as nickel, lead, molybdenum, cobalt, aluminum and steel in various media [19]–[21]. However, there is no report to our knowledge on the influence of side chain structure of glycine ($\text{R} = -\text{H}$), alanine ($\text{R} = -\text{CH}_3$) and phenylalanine ($-\text{CH}_2\text{Ph}$) on the inhibitive performance of the amino acids against metal corrosion. The interaction between inhibitors and metal surface was simulated by molecular dynamics whereas analysis of the electronic structures and

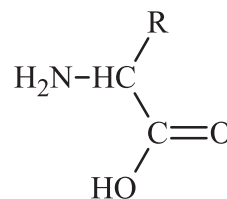


Figure 1: Molecular structures of α -amino acids used in the study. Where $\text{R} = -\text{H}$ for glycine; $\text{R} = -\text{CH}_3$ for alanine; $\text{R} = -\text{CH}_2\text{Ph}$ for phenylalanine.

energetics of the inhibitor molecules and substrate surface was achieved using density functional theory (DFT).

2 Materials and Methods

2.1 Materials

Glycine was supplied by Fischer Scientific Apparatus (Loughborough, England). Alanine was obtained from Aldrich Chemical Co. Ltd (Gillingham, England) while phenylalanine was obtained from BDH Chemicals Ltd (Poole, England). Having 99% purity, these amino acids were used without further purification. Their chemical structures differ in the side chain as displayed in Figure 1. The aluminium plates used in the study composed of 98.7Al, 0.5Fe and 0.48Si, and traces of Ti(0.005), V(0.016), Mn(0.012), Ni(0.013), Cu(0.048), Ga(0.013), Cl(0.014), K(0.04), Ca(0.01), In(0.10), Te(0.01), Ba(0.009), and Ir(0.03), falling within the wrought aluminium class (Vargel, 2004). Prior to corrosion experiments, all metal coupons were degreased in ethanol, rinsed with diethyl ether, air dried and preserved in a desiccator. Test solutions were prepared by diluting 37% HCl from Sigma-Aldrich in doubly distilled water.

2.2 Mass loss measurements

Aluminium specimens ($5.0 \text{ cm} \times 4.0 \text{ cm} \times 0.11 \text{ cm}$) were weighed, immersed each in 80 mL of a 0.3 M HCl solution containing different concentrations of inhibitor (0.0, 0.2, 0.4, and 0.6 g/L). Contact was allowed for 4 h at 303, 313 or 323 K. The coupons were withdrawn at a predetermined interval of time, washed, rinsed in diethyl ether, dried and reweighed. The mass losses were recorded. Each experiment was carried out three times. The mass measurements were performed



on Mettler FA2004 electronic balance. From the mass loss data, corrosion rate (CR , in $gh^{-1}cm^{-2}$), the degree of surface coverage (θ) and percentage degree of surface coverage I (%) were computed using Equations (1) to (3), respectively.

$$CR (gh^{-1}cm^{-2}) = \frac{\Delta m}{At} \quad (1)$$

$$\theta = 1 - \frac{m}{m_o} \quad (2)$$

$$I(\%) = \left(1 - \frac{m}{m_o}\right) \times 100 \quad (3)$$

Where m and m_o are the masses (g) of Al in the presence and absence of the inhibitor in HCl solution, Δm is the mass loss after 4 h, θ is the degree of surface coverage of the inhibitor, A is the area of the Al coupon (cm^2), t is the immersion time (h).

2.3 Electrochemical measurements

Linear polarization resistance (LPR) measurements were performed in 0.3 M HCl at 303 K using Model 668 AUTOLAB Potentiostat, having an acquisition system installed with NOVA software package version 1.8 and a three-electrode electrochemical cell: the aluminium coupon of surface area $1 cm^2$ as working electrode, an Ag/AgCl reference electrode and a graphite counter electrode. The aluminium metal was polarised between $-1,000$ and $2,000$ mV at scan rate of $0.333 mV s^{-1}$ and 303 K. From the polarization curves, Tafel slopes, corrosion potential and corrosion current were calculated. The inhibitor efficiency IE (%) was calculated using the formula [Equation (4)]:

$$IE(\%) = \left(\frac{CR_o - CR}{CR_o}\right) \times 100 \quad (4)$$

Where CR_o and CR are corrosion rates of the aluminium in aggressive environment with and without inhibitors, respectively.

2.4 Quantum chemical calculations

In order to study the effect of the molecular structure on inhibition efficiency, quantum chemical calculations with complete geometry optimizations of the corrosion inhibitors was performed using DMol³ module of Materials

Studio software version 8.0 (BIOVIA, Accelrys). This module is an atomic orbital implementation of density functional theory (DFT) in the local density approximation (LDA) regime. Calculations were done in the Perdew-Wang Correlation (PWC) form, at the double numerical quality plus d-functions (DND) atomic basis set level. Complete geometrical optimizations of Gly, Ala and Phe structures, the electron density, the highest occupied molecular orbital (HOMO), and the lowest unoccupied molecular orbital (LUMO) were obtained.

2.5 Molecular dynamic simulations

The molecular dynamics construction of unit cells and optimisation were performed using Forcite plus forcefield in the Accelrys Material Studio 8.0 software. The Al was cleaved along the densely packed reflection (Al (110)) being the most stable reflection compared to the open Al (111) and Al (100) planes. Forcite quench molecular dynamics was applied to sample low energy configurations of adsorbed amino acid molecules on the aluminium surface. Calculations were carried out in 5000 steps within simulation time of 5 ps invoking a 3×2 supercell at 350 K.

2.6 Surface characterisation

In order to understand the type of corrosion, aluminium coupons were immersed in 80 ml of 0.3 M HCl solution for 4 h in the presence or absence of the inhibitors at 303 K. The resulting surfaces were examined on Phenom ProX model (Netherlands) scanning electron microscope at accelerating voltages of 5.00 kV. Infrared Spectra of the adsorbed inhibitors were recorded using SHIMADZU FTIR-8400S Fourier Transform Infrared Spectrometer (FTIR) over a frequency range of $400-4000 cm^{-1}$. Elemental analysis of aluminium test plates was performed on Mini pal 4 PW 4030 energy dispersive X-ray fluorescence spectrometer (EDXRF) installed with Mini Pal analytical software. The specimens were stimulated by a potential of 30 kV and a current of 1 mA for 10 min.

3 Results and Discussion

3.1 Mass loss analysis

The inhibition performance profile of Phe for the

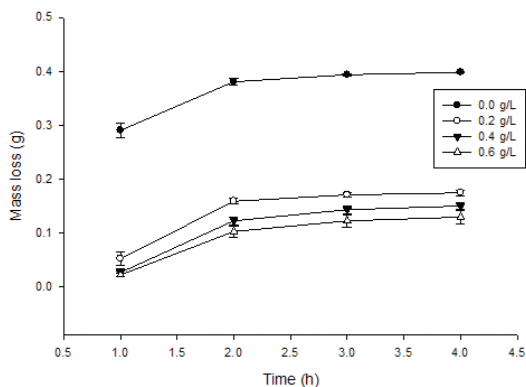


Figure 2: Effect of varying Phe concentration on the corrosion inhibition of aluminium coupons in 0.3 M HCl solution at 303 K. Error bars are standard deviations.

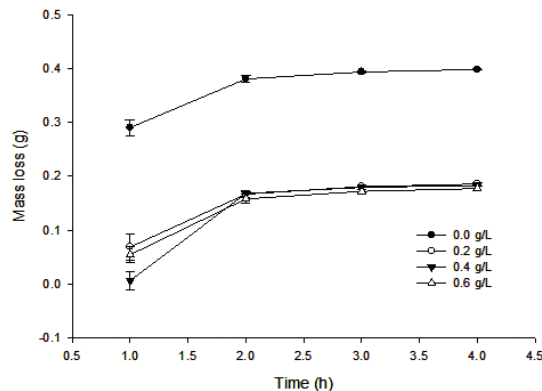


Figure 3: Effect of varying Ala concentration on the corrosion inhibition of aluminium in 0.3 M HCl solution at 303 K.

anti-corrosion of aluminium samples in 0.3 M HCl media at 303 K is shown in Figure 2. As seen from this figure, aluminium mass loss decreases as the concentration of Phe is increased from 0.0 to 0.6 g/L. Accordingly, Ala showed the same behaviour under the same conditions (Figure 3). This observation implies a decline in corrosion rate as the inhibitor concentration is increased and can be attributed to the reduced direct contact of the metal with the corrosive environment with adsorption of the inhibitor molecules. A similar observation was made by several workers. Zhao *et al.* [9] for example, observed increasing anti-corrosion efficiency of triazenedithiols on aluminium corrosion until nearly 100%.

It can be observed from Figures 2 and 3 that regardless of the inhibitor dose applied, Ala exhibits relatively lower mass loss compared to Phe indicating clearly its superior anti-corrosion efficiency. In both

cases, however, corrosion was more rapid in the first 2 h of contact with the acid. This may be attributed to the breakdown of the air-formed passive film and the initiation of pitting, which is traditionally followed by steady state corrosion conditions, due to cathodic reaction [22], [23].

The results of amino acid inhibition against aluminium mass losses in 0.3 M HCl solution at 313 and 323 K are presented in Table 1. It can readily be gathered from the table that the corrosion aluminium declines with doses of Gly, Ala or Phe at these temperatures. As observed, the higher the concentration of inhibitor the higher the inhibition efficiency. However, for each inhibitor dose, aluminium was found not to deteriorate faster in presence of Phe than either Gly or Ala. This stage presupposes that as the temperature of the aggressive solution is slightly increased from the foregoing 303 K, the Phe desorbs at a slower rate than either of Gly or Ala.

Table 1: Mass losses of aluminium in 0.3 M HCl at 4 h and 313, and 323 K

Inhibitor	Concentration (g/L)	Mass loss (g) at 313 K	IE (%)	Mass loss (g) at 323 K	IE (%)
None	-	0.4127 ± 0.0023	0	0.4216 ± 0.0023	0
Gly	0.2	0.1900 ± 0.0040	54	0.2026 ± 0.0012	52
	0.4	0.1811 ± 0.0020	55	0.1930 ± 0.0002	54
	0.6	0.1739 ± 0.0051	56	0.1896 ± 0.0026	55
Ala	0.2	0.1912 ± 0.0007	54	0.2072 ± 0.0001	51
	0.4	0.1860 ± 0.0007	55	0.2059 ± 0.0011	51
	0.6	0.1818 ± 0.0022	56	0.1980 ± 0.0010	53
Phe	0.2	0.1767 ± 0.0051	57	0.1976 ± 0.0013	53
	0.4	0.1644 ± 0.0031	60	0.1889 ± 0.0020	55
	0.6	0.1593 ± 0.0013	62	0.1790 ± 0.0058	57

3.2 Activation parameters

The apparent activation energy (E_{ads}) for aluminium corrosion in HCl in the absence and presence of Gly, Ala and Phe, adsorption entropy (ΔS_{ads}) and enthalpy of adsorption (ΔH_{ads}) were calculated using the Arrhenius equation [Equation (5)] and activated state equation [Equation (6)].

$$CR = A e^{\frac{-E_{ads}}{RT}} \quad (5)$$

$$\frac{CR}{T} = \frac{R}{N_A h} e^{\frac{\Delta S_{ads}}{R}} e^{\frac{-H_{ads}}{RT}} \quad (6)$$

Where CR is the corrosion rate, A is the pre-exponential factor, T is the absolute temperature (K), R is the molar gas constant (8.3142 J/mol K), N_A is the Avogadro's constant and h is Planck's constant (6.621×10^{-34} Js). By taking the natural logarithm of Equation (5) [or Equation (6)] $\ln CR$ (or $\ln CR/T$) can be plotted against $1/T$ which will give straight line with slope $\Delta E_{ads}/R$ (or $\Delta H_{ads}/R$), and intercept equal to $\ln A$ (or $\ln(R/N_A h) + (\Delta S_{ads}/R)$, respectively). The average calculated values of ΔE_{ads} , ΔS_{ads} and ΔH_{ads} are presented in Table 2. The ΔE_{ads} and ΔH_{ads} values are small and positive, indicating physical adsorption and endothermic aluminium dissolution, respectively. In the same way, the lower values of ΔE_{ads} of the inhibited systems compared to the uninhibited system reveal physical adsorption [18]. The inhibition can be said to be diffusion-controlled due to the characteristic low thresholds of energy displayed. However, in this case, the data show that ΔE_{ads} is not a function of inhibitor concentration.

Table 2: Activation parameters for aluminium corrosion in 0.3 HCl solutions at 303 K

Aggressive solution	ΔE_{ads} (kJ/mol)	ΔH_{ads} (kJ/mol)	ΔS_{ads} (kJ/mol K)
Devoid of inhibitor	2.33	-0.269	-0.290
With 0.2g/L Gly	3.74	1.129	-0.292
With 0.4g/L Gly	3.31	0.756	-0.293
With 0.6g/L Gly	3.71	1.074	-0.293
With 0.2g/L Ala	4.05	2.452	-0.291
With 0.4g/L Ala	4.74	6.794	-0.289
With 0.6g/L Ala	4.48	10.812	-0.300
With 0.2g/L Phe	5.09	2.452	-0.288
With 0.4g/L Phe	9.43	6.794	-0.274
With 0.6g/L Phe	13.36	10.812	-0.262

The values of ΔS_{ads} (Table 2) were all negative due to poor freedom of the inhibitor molecules on the aluminium surface. Alanine has the highest negative values of this parameter (-0.291 to -0.300 kJ/mol K), indicating a great order of the adsorption onto the aluminium pits [24]. These observations reveal further that the aromatic ring of Phe side chain (or proton of Gly, which is a given) do not favour inhibition efficiency compared. Interestingly, the values of ΔH_{ads} for aluminium corrosion with or without 0.2 g/L of Ala and Phe are very close to RT ($\Delta H_{ads} \approx RT = 2.52$ kJ/mol at 303 K). This reflects the characteristics of liquid or solid reactions [25], likely to be aluminium dissolution due to ineffective inhibition.

3.3 Adsorption isotherms

The adsorption process is usually described by the adsorption isotherm. Attempts by various workers to describe inhibitor adsorption has been made by invoking several adsorption isotherms such as Langmuir, Frumkin, Hill de Boer, Parsons, Temkin, Flory-Huggins, Dhar-Flory-Huggins, Bockris-Swinkels and El-Awady *et al.* and Freundlich [3], [17]. In this study, data were fitted to Langmuir, Temkin, Flory-Huggins and El-Awady isotherms. Eventually, the Langmuir isotherm, described by Equation (7), was found to consistently hold true.

$$\frac{C}{\theta} = \frac{1}{K_{ads}} + C \quad (7)$$

Where C is the inhibitor concentration (g/L), K_{ads} is the adsorptive equilibrium constant. A plot of C/θ against C gives a straight line with intercept $1/K_{ads}$. The K_{ads} values permitted the calculation of free energy change (ΔG_{ads}°) from Equation (8).

$$\ln K_{ads} = \ln \frac{1}{55.5} - \frac{\Delta G^{\circ}}{RT} \quad (8)$$

Where 55.5 is the molar concentration of water in solution (mol/L), R and T are as described above. Values of ΔG_{ads}° and K_{ads} are displayed in Table 3. The Langmuir adsorption model gave very high linear correlation values (> 0.99). Generally, from the table, the values of ΔG_{ads}° are negative and lower than -20 kJmol $^{-1}$, so the adsorption is consistent with physisorption, resulting from electrostatic attraction

Table 3: Equilibrium data for the adsorption of inhibitors on Al surface

Inhibitor	At 303 K				At 313 K			
	ΔG_{ads}° (kJ/mol)	ΔK^{ads} (M ⁻¹)	Slope	R ²	ΔG_{ads}° (kJ/mol)	ΔK^{ads} (M ⁻¹)	Slope	R ²
Gly	-8.763	0.584	0.946	0.9995	-9.070	0.588	0.946	0.9996
	-8.754	0.582	0.949	0.9999	-9.109	0.597	0.926	0.9998
	-8.706	0.571	0.962	0.9999	-8.975	0.567	0.984	0.9996
Ala	-8.733	0.577	0.943	0.9993	-9.034	0.580	0.955	0.9999
	-8.616	0.551	0.988	1.000	-8.975	0.567	0.961	1.0000
	-8.621	0.552	0.978	0.9998	-8.957	0.563	0.972	1.0000
Phe	-8.767	0.585	0.991	0.9956	-9.335	0.651	0.912	0.9992
	-8.630	0.554	0.978	0.9988	-9.241	0.628	0.941	0.9997
	-8.621	0.552	0.978	0.9967	-9.249	0.630	0.950	1.000

Table 4: Linear polarization data for aluminium corrosion in 0.3 M HCl acid solutions in the presence and absence of inhibitors at 303K

Al + HCl _(aq)	E_{corr} (V)	i_{corr} (Acm ⁻²)	β_a (Vdec ⁻¹)	β_c (Vdec ⁻¹)	CR (mmyr ⁻¹)	IE (%)
Devoid of inhibitor	-0.91094	1.53 x 10 ⁻⁵	0.18218	0.88364	5.8475	0
With 0.6g/L Gly	-1.06230	1.55 x 10 ⁻⁴	0.27811	0.16131	0.5567	90
With 0.6g/L Ala	-1.08370	1.01 x 10 ⁻⁴	0.14980	0.08826	0.3668	94
With 0.6g/L Phe	-0.97720	2.99 x 10 ⁻⁴	0.26266	0.13419	1.0851	81

between charged aluminium surface and charged species in the solution [26]. The adsorption of all of the inhibitors occurred with small values of K_{ads} which further confirms physical adsorption.

3.4 Potentiodynamic polarisation profiling

Potentiodynamic polarisation techniques are widely used to investigate the type, behaviour, extent and rate of electrochemical corrosion. Table 4 shows the linear polarisation data obtained for aluminium corrosion in 0.3 M HCl with or without Gly, Ala or Phe.

The shifts in corrosion potential (E_{corr}) were negative irrespective of the amino acid used (Table 4). The highest corrosion rate (CR) and E_{corr} values were obtained from the aluminium-HCl system without inhibitor. Generally, in both the mass loss and potentiodynamic polarisation studies, the inhibition efficiency (IE) values reached maximum with of 0.6 g/L amino acid. All of the amino acid inhibitors showed large negative shifts in E_{corr} (> 0.085 V) confirming cathodic control [24]. The lowest shift was obtained with 0.6 g/L phenylalanine which corresponds to the lowest inhibition efficiency (81%) while the highest anti-corrosion efficiency (IE = 94%) and the lowest cathodic Tafel slope (β_c , 0.08826 Vdec⁻¹) were obtained with Ala.

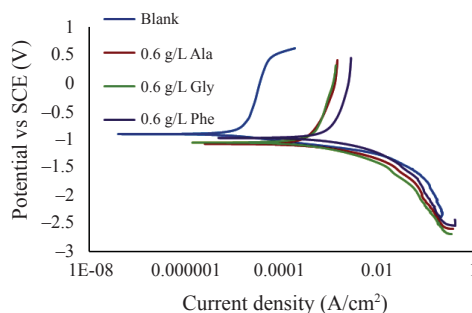


Figure 4: Tafel polarization curves for the corrosion of aluminium in 0.3M HCl solution containing 0.6 g/L Ala, Gly and Phe at 303 K.

The polarisation profiles of aluminium in 0.3 M hydrochloric acid with 0.6 g/L of Ala, Gly and Phe is shown in Figure 4. The electropotentials range from -0.91 to -1.18 V and are more negative than those reported for flowing, aerated water, 0.5 to -0.8 V [11]. This is therefore revelatory of the severity of the corrosion in hydrochloric acid regimes of the study.

3.5 Scanning electron microscopy

In order to study the changes in the aluminium with corrosion, scanning electron microscopy was performed.

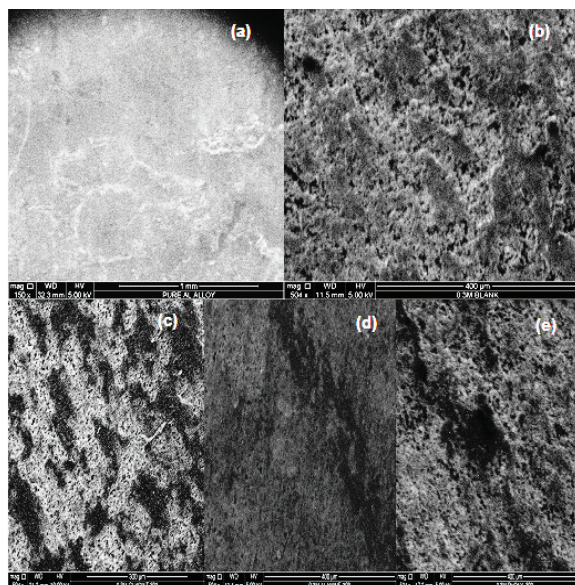
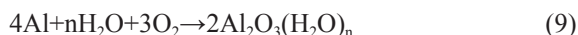


Figure 5: Scanning electron micrographs of (a) Pure aluminium (b) aluminium in 0.3 M HCl (c) aluminium in 0.3 M HCl + 0.6 g/L Gly at 303 K (d) aluminium in 0.3 M HCl + 0.6 g/L Ala at 303 K (e) aluminium in 0.3 M HCl + 0.6 g/L Phe at 303 K.

Micrographs obtained for different corrosion systems are shown in Figure 5(a) to (e). The development of incongruent pits on the regular aluminium surface [Figure 5(a)] and overall structural deterioration can be seen in Figure 5(b) due of contact with 0.3 M hydrochloric acid media for 4 h. This corrosion was inhibited by the addition of 0.6 g/L amino acids and pits were geometrically blocked. The extent of the blockage depends upon the amino acid used. Glycine [Figure 5(c)] and Phe [Figure 5(e)] were less efficient in the blockage of the pits when compared with Ala [Figure 5(d)] perhaps as a result of their poor efficiency of cathodic inhibition. The adsorbed inhibitor film is clearly visible upon juxtaposing the pit-stricken aluminium in 0.3 M HCl devoid of inhibitor [Figure 5(b)] and the one in presence of Ala which barely shows no pits or cracks [Figure 5(d)]. The order of this geometric blocking of the active surface sites and lessening of surficial roughness varies with amino acids as Ala > Phe > Gly. This order further shows that the effect of the aromatic side chain of Phe does not dominate over the effect of alkyl groups of Ala.

3.6 Mechanism of inhibition

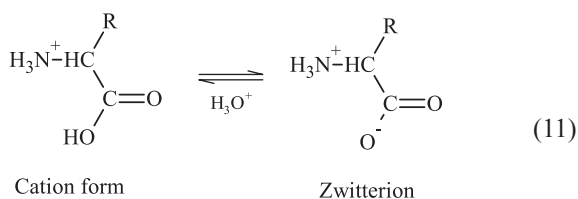
Naturally, the test aluminium plates prior to use in the study have air passive film of aluminium oxide on their surface due to oxidation as shown in Equation (9).



However, the continuous dissolution of aluminium in presence of an aggressive electrolyte solution or under applied bias can be represented by Equation (10).



Basically, Gly, Ala and Phe used in this study are known to exist in cationic form at very low pH [27]. Any Arrhenius acids such as HCl will protonate amino acid so that it will remain in cationic form rather than the dipolar ion as suggested by Equation (11). The cationic form will be stable as predicted by Le Châtlier's principle. As a rule, the Al^{3+} will be repelled by the NH_3^+ being like charged. In acidic medium, only the other functional groups ($-\text{OH}$, $-\text{COOH}$) of the amino acids can therefore participate in the adsorption. As described in the previous section the adsorption proceeds by physical interactions between the aluminium surface and these functionalized contacts. The contact zones are further proposed by the below-proceeding studies.



3.7 Quantum chemical calculations

Quantum chemical calculations were performed using LDA-DFT/PWC/DND level of theory with the DMol³ program to further elucidate the inhibition mechanism. The values of inhibition parameters are displayed in Table 5. It is well known that the higher the E_{HOMO} edge, the higher the ability of a molecule to donate electrons to lower-energy acceptor molecules [28]. The reverse is the case for E_{LUMO} .

The frontier molecular orbital diagrams of Gly, Ala and Phe exhibiting these energies are presented in

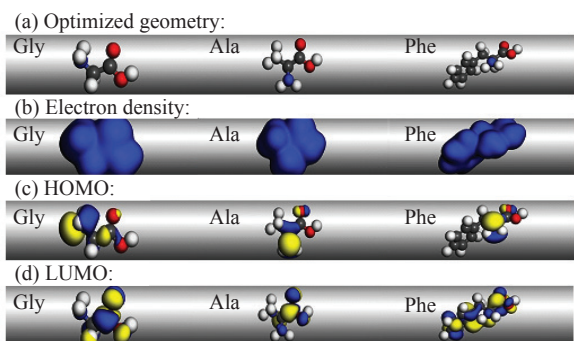


Figure 6: Frontier molecular orbital density and optimised structures of Gly, Ala and Phe from left to right respectively showing: (a) Structures (b) Total electron density (c) HOMO (d) LUMO. Colour scheme: White = H, blue = N, red = oxygen, grey = carbon.

Figure 6. It would be seen from Table 5 that the E_{HOMO} value of Ala was found to be the least (-5.559 eV), which makes it highly electron-donating, susceptible to electrostatic attraction in the Al^{3+} environment and an excellent corrosion inhibitor. The superiority of inhibition can also be related to the value of the fraction of electrons transferred (ΔN). This important parameter is based on absolute electronegativity of both the metal and the inhibitor and their absolute hardness. A higher

value of ΔN is an evidence for relatively stronger electron donation and a higher tendency to interact with the aluminium [29]. Interestingly from Table 4, Ala exhibits the highest ΔN value (0.5098) due to its stronger electron donation.

In this study, Ala was found to be the most efficient inhibitor for aluminium corrosion and physisorption mechanism has been confirmed. From Table 5, this compound has a lower energy gap (ΔE) than Phe, and a value very close to Gly. However, because physical adsorption holds the combination of values of E_{HOMO} and ΔN is more important than the energy gap.

In order to further investigate the local reactivity of the inhibitors due to different amino functional groups, the Fukui indices were calculated ab initio using DMol³ Mulliken analysis of Materials Studio 8 (Table 6). The electrophilic and nucleophilic attack sites were represented by Fukui descriptors F^- and F^+ , respectively. It can be seen from Table 6 that the electrophilic indices of Gly and Phe are oriented around the nitrogen atom N(5) and N(10) while that of Ala is centred around the oxygen atom O(5). This reveals that oxygen of is the zone by which the adsorption of Ala takes place [30]. The nitrogen will not be used for the adsorption perhaps because of electrostatic repulsion between amino acid-based NH_3^+ and with Al^{3+} .

Table 5: Values of electronic parameters and eigenvalues of Gly, Ala and Phe

Electronic/structural property	Gly	Ala	Phe
HOMO (at orbital number)	20	24	44
LUMO (at orbital number)	21	25	45
E_{HOMO} (eV)	-5.871	-5.559	-5.642
E_{LUMO} (eV)	-1.292	-1.365	-1.453
ΔE (eV)	4.579	4.194	4.189
Molecular mass (g/mol)	75.067000	89.093800	165.191400
Ionization potential (IP) (eV)	5.871	1.365	1.453
Electron affinity (EA) (eV)	1.292	1.365	1.453
Absolute/Global hardness (η)	2.2895	2.0970	2.0945
Global softness (σ)	0.4368	0.4769	0.4774
Absolute electronegativity (χ)	3.5815	3.4620	3.5475
Total number of electrons	40.0	48.0	88.0
Fraction of electrons transferred (ΔN)	0.4408	0.5098	0.4900

Table 6: Calculated Fukui Indices for Gly, Ala and Phe

Inhibitor molecule	Electrophilic (F^-)				Nucleophilic (F^+)			
	Mulliken		Hirshfeld		Mulliken		Hirshfeld	
	Atom	Value	Atom	Value	Atom	Value	Atom	Value
Gly	N(5)	0.353	N(5)	0.358	C(2)	0.248	O(4)	0.230
Ala	O(5)	0.342	O(5)	0.342	C(3)	0.231	O(5)	0.217
Phe	N(10)	0.317	N(10)	0.308	C(9)	0.109	O(11)	0.106

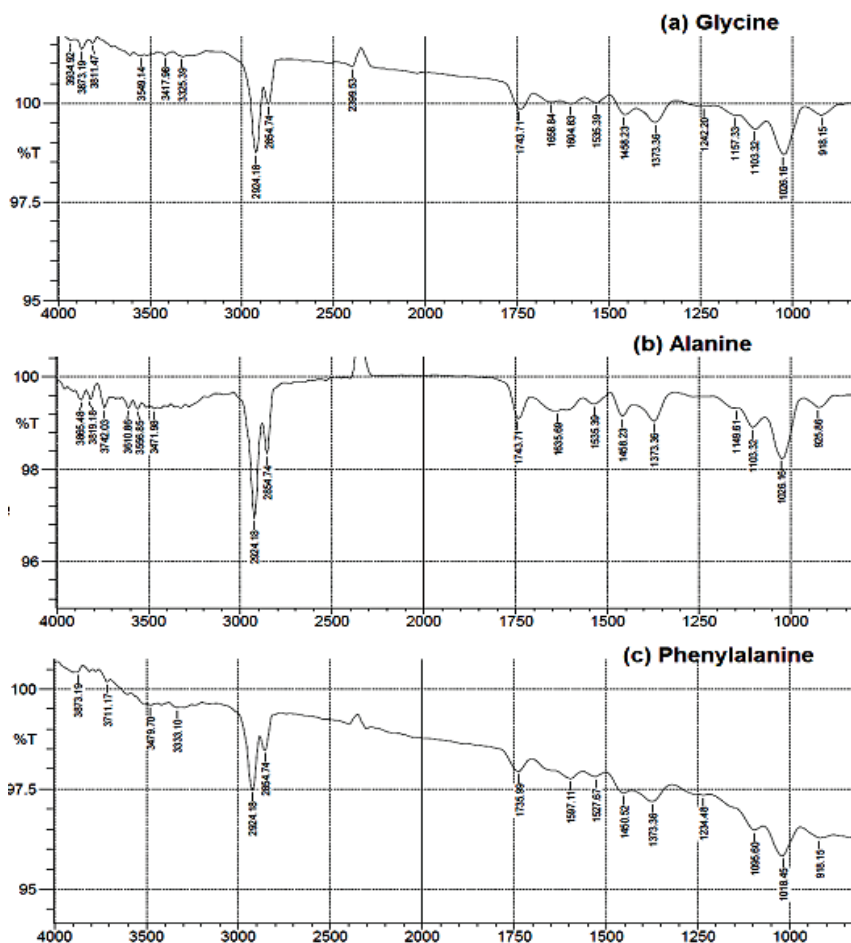


Figure 7: FTIR spectra of the 0.6 g/L Gly amino acids after aluminium corrosion inhibition in hydrochloric acid at 323 K.

3.8 Fourier transform IR analysis

The FTIR spectra of amino acid groups on the surface of aluminium are shown in Figure 7. The appearance of a peak at 3455 cm^{-1} is due to the phenyl ring of Phe. The vibrational peak at $\approx 1635\text{ cm}^{-1}$ represents -C=O group while -NH group constantly occurs at 29131.90 cm^{-1} . The ammonia cation (NH_3^+) is evidenced by the broad band spanning $3050\text{-}2675\text{ cm}^{-1}$. The weak broad peak at 3464 cm^{-1} may be assigned to the intermolecular hydrogen bonding stretching mode of O-H . From the FTIR spectra, there is no evidence of bonding of the aluminium with any of the amino acids. This reaffirms that the mechanism is physical adsorption.

3.9 Adsorption behaviour of inhibitors

Molecular dynamics is widely used to investigate the adsorption behaviour of the inhibitors on aluminium surface [31]–[33]. In this study, Forcite quench molecular dynamics of Materials Studio 8 was utilised. Figure 8 shows the cross-sectional side views of the lowest energy adsorption configurations for monomolecular and multimolecular inhibitor amino acids on Al (110) plane. Upon comparison of the three monomolecular amino acid configurations in the adsorbed phase [Figure 7(a)], it can be clearly seen that each of them can be adsorbed on the aluminium surface through the nitrogen atoms. However, the multi-molecular adsorption of Gly and Ala takes place through O atom

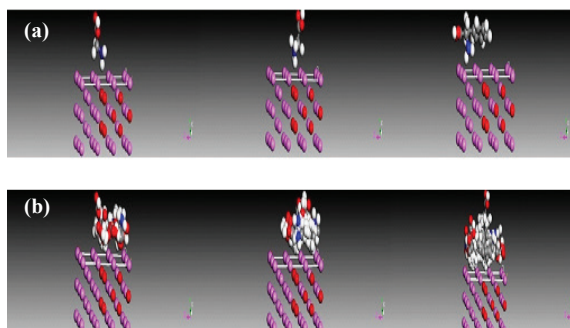


Figure 8: The final side snapshots of adsorbed Gly Ala and Phe molecules, from left to right respectively, on aluminium (110) reflection. (a) Single molecules. (b) Many molecules.

while for Phe, huge clusters of C atoms appear to compete with the oxygen for the active sites [Figure 7(b)].

Colour scheme: White = H, blue = N, red = oxygen, grey = carbon.

To quantitatively estimate the interaction between the amino acids and the aluminium surface, the theoretical adsorption energy, E_{ads} , was calculated using Equation (12) below:

$$E_{ads} = E_{total} - (E_{inhibitor} + E_{Al\ surface}) \quad (12)$$

Where $E_{inhibitor}$, $E_{Al\ surface}$ and E_{total} correspond to the total energies of the inhibitor molecule, Al (110) plane and the adsorbed molecule coupled with gas phase Al (110), respectively. In this study, the metal surface energy was zeroed. Parameters calculated such as kinetic energy, potential energy, the energy of the inhibitor molecule and energy of Al (110) surface and binding energy, are presented in Table 6. Basically, the more negative the value of binding energy the more

stable the adsorption structure [34]. The high negative binding energies account for the good performance of amino acids as inhibitors. Even though Phe has the highest binding energy (−36.95170019 kcal/mol) and expectedly more stability, lower corrosion rate was obtained with this compound compared Ala because the adsorption mechanism is physisorption. In addition, there is a possibility of steric hindrance of the adsorption zones by the toluoyl side chain of the Phe [26].

4 Conclusions

The influence of glycine, alanine and phenylalanine side chains on corrosion inhibition of aluminium in hydrochloric acid was investigated successfully from various viewpoints. Alanine showed the highest inhibition efficiency. The side chain structure of these α -amino acids was found to show no effect on inhibition efficiency in acidic media. Results obtained from mass loss, thermodynamics and theoretical studies support these observations. Based on Tafel electropotential profiles alanine showed the highest inhibition efficiency. Scanning electron micrographs confirm the uniform blockage of etched sites on acid-stricken aluminium slabs. The zone of inhibition of alanine was confirmed to be oxygen. As the adsorption followed physisorption, the combination of high energy gap, aromatic side chain, π bonds and binding energy obtained of phenylalanine did not positively influence its efficiency over alanine.

Acknowledgments

Shehu N.U. extends his sincere appreciation to David Arthur Ebuka, Ahmadu Bello University, Zaria for support on simulations.

Table 6: Values of adsorption parameters for the interaction of Gly, Ala and Phe with the Al (110) surface using Forcite quench dynamics

Adsorption Properties (kcal/mol)	Gly	Ala	Phe
Total kinetic energy	10.43282176	13.56266829	23.99549006
Total potential energy	11.77826517	−0.37687297	−14.28589205
Energy of molecule	25.40314257	18.22309314	22.66580814
Energy of Al(110) surface	0.00000000	0.00000000	0.00000000
Binding energy	−13.62487740	−18.59996611	−36.95170019



References

- [1] D. E. J. Talbot and J. D. R. Talbot, *Corrosion Science and Technology*, 3rd ed. New York: Taylor and Francis, 2018, pp. 159–194.
- [2] M. Goyal, S. Kumar, I. Bahadur, C. Verma, and E. E. Ebenso, “Organic corrosion inhibitors for industrial cleaning of ferrous and non-ferrous metals in acidic solutions: A review,” *Journal of Molecular Liquids*, vol. 256, pp. 565–573, Apr. 2018.
- [3] S. Deng, X. Li, and H. Fu, “Acid violet 6B as a novel corrosion inhibitor for cold rolled steel in hydrochloric acid solution,” *Corrosion Science*, vol. 54, no. 2, pp. 760–768, 2011.
- [4] K. Tebbji, N. Faska, A. Tounsi, and H. Oudda, “The effect of some lactones as inhibitors for the corrosion of mild steel in 1M hydrochloric acid,” *Materials Chemistry and Physics*, vol. 106, no. 2–3, pp. 260–267, 2007.
- [5] S. L. Priya, A. Chitra, S. Rajendran, and K. Anuradha, “Corrosion behaviour of aluminium in rain water containing garlic extract,” *Surface Engineering*, vol. 21, no. 3, pp. 229–231, 2005.
- [6] C. Vargel, *Corrosion of Aluminium*. Amsterdam: Elsevier Ltd, 2018, pp. 185–207.
- [7] R. Zandi-zand, A. Ershad-langroudi, and A. Rahimi, “Organic–inorganic hybrid coatings for corrosion protection of 1050 aluminum alloy,” *Journal of Non-Crystalline Solids*, vol. 351, no. 14–15, pp. 1307–1311, 2005
- [8] R. Rosliza, A. Nora’aini, and W. B. Wan Nik, “Study on the effect of vanillin on the corrosion inhibition of aluminum alloy,” *Journal of Applied Electrochemistry*, vol. 40, no. 4, pp. 833–840, 2010.
- [9] P. Arellanes-Lazoda, O. Olivares-Xometl, D. Guzmán-Lucero, N. V. Likhanova, and M. A. Domínguez-Aguilar, I. V. Lijanova, E. Arce-Estrada, “The inhibition of aluminum corrosion in sulfuric acid by poly(1-vinyl-3-alkyl-imidazolium hexafluorophosphate),” *Molecules*, vol. 7, no. 8, pp. 5711–5734, 2014.
- [10] E. Li, J. Wu, D. Zhang, Y. Sun, and J. Chen, “D-phenylalanine inhibits the corrosion of Q235 carbon steel caused by *Desulfovibrio sp.*,” *International Biodeterioration & Biodegradation*, vol. 127, pp. 178–184, 2018.
- [11] Q. Zhao, T. Tang, P. Dang, Z. Zhang, and F. Wang, “The corrosion inhibition effect of triazinedithiol inhibitors for aluminium alloy in a 1M HCl solution,” *Metals*, vol. 7, no. 2, pp. 1–11, 2017.
- [12] D. Landolt, *Corrosion and Surface Chemistry of Metals*. Switzerland: EPFL Press, 2007, pp. 548–550.
- [13] I. B. Obot and N. O. Obi-Egbedi, “Anti-corrosive properties of xanthone on mild steel corrosion in sulphuric acid: Experimental and theoretical investigations,” *Current Applied Physics*, vol. 11, no. 3, pp. 382–392, 2011.
- [14] A. S. Patel, V. A. Panchal, G. V. Mudaliar, and N. K. Shah, “Impedance spectroscopic study of corrosion inhibition of Al-Pure by organic Schiff base in hydrochloric acid,” *Journal of Saudi Chemical Society*, vol. 17, no. 1, pp. 53–59, 2013.
- [15] A. K. Satapathy, G. Gunasekaran, S. C. Sahoo, K. Amit, and P. V. Rodriguez, “Corrosion inhibition by *Justicia gendarussa* plant extract in hydrochloric acid solution,” *Corrosion Science*, vol. 51, no. 12, pp. 2848–2856, 2009.
- [16] S. Rajendran, J. Jeyasundari, P. Usha, J. A. Selvi, B. Narayanasamy, A. P. P. Regis, and P. Rengan, “Corrosion behaviour of aluminium in the presence of an aqueous extract of Hibiscus Rosa-sinensis,” *Portugaliae Electrochimica Acta*, vol. 27, no. 2, pp. 153–164, 2009.
- [17] Y. Qiang, S. Zhang, B. Tan, and S. Chen, “Evaluation of Ginkgo leaf extract as an eco-friendly corrosion inhibitor of X70 steel in HCl solution,” *Corrosion Science*, vol. 133, pp. 6–18, 2018.
- [18] L. Hamadi, S. Mansouri, K. Oulmi, and A. Kereche, “The use of amino acids as corrosion inhibitors for metals: A review,” *Egyptian Journal of Petroleum*, vol. 27, no. 4, pp. 1157–1165, 2018.
- [19] C. Zhu, H. X. Yang, Y. Z. Wang, D. Q. Zhang, Y. Chen, and L. X. Gao, “Synergistic effect between glutamic acid and rare earth cerium (III) as corrosion inhibitors on AA5052 aluminum alloy in neutral chloride medium,” *Ionics*, vol. 25, no. 3, pp. 1395–1406, 2018.
- [20] J. Bao, H. Zhang, X. Zhao, and J. Deng, “Biomass polymeric microspheres containing aldehyde groups: Immobilizing and controlled-releasing amino acids as green metal corrosion inhibitor,” *Chemical Engineering Journal*, vol. 341, pp. 146–156, 2018.

- [21] Z. Shi, M. Liu, and S. Atrens, “Measurement of the corrosion rate of magnesium alloys using Tafel extrapolation,” *Corrosion Science*, vol. 52, no. 2, pp. 579–588, 2010.
- [22] V. Cicek and B. Al-Numan, *Corrosion Chemistry*. United States of America: Scrivener Publishing LLC & Wiley & Sons, 2011, pp. 7–14.
- [23] E. S. Ferreira, C. Giacomelli, and A. Spinelli, “Evaluation of the inhibitor effect of l-ascorbic acid on the corrosion of mild steel,” *Materials Chemistry and Physics*, vol. 83, no. 1, pp. 129–134, 2004.
- [24] E. A. Noor, “Evaluation of inhibitive action of some quaternary n-heterocyclic compounds on the corrosion of Al–Cu alloy in hydrochloric acid,” *Materials Chemistry and Physics*, vol. 114, no. 2–3, pp. 533–541, 2009.
- [25] T. Engel and P. Reid, *Physical Chemistry*. San Francisco: Pearson Education, 2006, pp. 925–926.
- [26] N. Soltani, N. Tavakkoli, M. Khayatkashani, and M. R. Jalali, “Green approach to corrosion inhibition of 304 stainless steel in hydrochloric acid solution by the extract of *Salvia officinalis* leaves,” *Corrosion Science*, vol. 62, no. pp. 122–135, 2012.
- [27] J. M. Hornback, *Organic Chemistry*. Taiwan: Thomson Brooks/Cole, 2006, pp. 1126.
- [28] L. Fragoza-Mar, O. Olivares-Xometl, M. A. Domínguez-Aguilar, E. A. Flores, P. Arellanes-Lozada, and F. Jiménez-Cruz, “Corrosion inhibitor activity of 1,3-diketone malonates for mild steel in aqueous hydrochloric acid solution,” *Corrosion Science*, vol. 61, pp. 171–184, 2012.
- [29] M. Dehdab, M. Shahraki, and S. M. Habibi-Khorassani, “Theoretical study of inhibition efficiencies of some amino acids on corrosion of carbon steel in acidic media: Green corrosion inhibitors,” *Amino Acids*, vol. 48, no. 1, pp. 291–306, 2015.
- [30] K. F. Khaled, “Corrosion control of copper in nitric acid solutions using some amino acids—A combined experimental and theoretical study,” *Corrosion Science*, vol. 52, no. 10, pp. 3225–3234, 2010.
- [31] S. Kaya, C. Kaya, L. Guo, F. Kandemirli, B. Tüzün, I. Uğurlu, L. H. Madkour, and M. Saraçoğlu, “Quantum chemical and molecular dynamics simulation studies on inhibition performances of some thiazole and thiadiazole derivatives against corrosion of iron,” *Journal of Molecular Liquids*, vol. 219, pp. 497–504, 2016.
- [32] L. Guo, S. Kaya, I. B. Obot, X. Zheng, and Y. Qiang, “Toward understanding the anticorrosive mechanism of some thiourea derivatives for carbon steel corrosion: A combined DFT and molecular dynamics investigation,” *Journal of Colloid and Interface Science*, vol. 506, pp. 478–485, 2017.
- [33] E. Alibakhshi, M. Ramezanzadeh, G. Bahlakeh, B. Ramezanzadeh, M. Mahdavian, and M. Motamedi, “*Glycyrrhiza glabra* leaves extract as a green corrosion inhibitor for mild steel in 1 M hydrochloric acid solution: Experimental, molecular dynamics, Monte Carlo and quantum mechanics study,” *Journal of Molecular Liquids*, vol. 255, pp. 185–198, 2018.
- [34] S. K. Saha, P. Gosh, A. Hens, and N. C. Murmu, “Density functional theory and molecular dynamics simulation study on corrosion inhibition performance of mild steel by mercapto-quinoline Schiff base corrosion inhibitor,” *Physica E: Low-dimensional Systems and Nanostructures*, vol. 66, pp. 332–341, 2015.